

# Applications of Fourier transform infrared microspectroscopy to the analysis of microscopic orientation in liquid crystalline polymer sheets

Akira Kaito, Mutsumasa Kyotani and Kazuo Nakayama

Research Institute for Polymers and Textiles, 1-1-4 Higashi, Tsukuba, Ibaraki 305, Japan

(Received 18 March 1991; revised 26 June 1991; accepted 1 July 1991)

Fourier transform infrared (*FTi.r.*) microspectroscopy was applied to evaluate the microscopic orientation of extrusion moulded sheets of a thermotropic liquid crystalline polymer, consisting of 4-hydroxybenzoic acid units, biphenol units and benzene dicarboxylic acid units. The polarized i.r. spectra were measured in the microscopic area down to 40  $\mu\text{m}$  using a redundantly apertured i.r. microscope equipped with a wire-grid polarizer. It was shown that Beer's law held in the absorbance range below 2.5, and the polarization properties of oriented samples were accurately measured by *FTi.r.* microspectroscopy. The orientation profiles of the polymer sheets were obtained by plotting the dichroic ratio of the 1602  $\text{cm}^{-1}$  band against distance from the centres of sheets. In the case of the sheet 0.68 mm thick, the central region is nearly isotropic, but the dichroic ratio increases markedly toward the surface of the sheet. In the thinner sheet (0.255 mm), the polymer chains in both surface and central regions are highly oriented in the extrusion direction, and the dichroic ratio gradually increases on approaching the surface. At the same sheet thickness, the degree of orientation decreases as the extrusion temperature is lowered. The orientation profiles obtained by polarized *FTi.r.* microspectroscopy are in accordance with the morphological structures studied by scanning electron microscopy.

(Keywords: *FTi.r.* microspectroscopy; molecular orientation; liquid crystalline polymer)

## INTRODUCTION

In recent years, Fourier transform infrared (*FTi.r.*) microspectroscopy has been extensively studied as an analytical tool for microscopic areas, such as contaminants or inhomogeneities in materials<sup>1,2</sup>, thin fibres<sup>1,3-5</sup> and thin layers in laminate films<sup>2,5,6</sup>. By a combination of *FTi.r.* spectroscopy with optical microscopy, infrared (i.r.) spectra with high signal-to-noise ratio can be measured for the microscopic area. Therefore, *FTi.r.* microspectroscopy provides valuable information on the molecular structure of samples in the microscopic domain. Furthermore, the polarization measurements of *FTi.r.* microspectroscopy have been discussed and the polarized microspectra of thin fibres reported<sup>1,3,7</sup>.

On the other hand, thermotropic liquid crystalline polymers can be processed from the melt by extrusion and injection mouldings. The structural distributions are sometimes formed inside the materials of liquid crystalline polymers as a result of complex flow of the polymer melt. A skin-core structure with a highly oriented skin layer and a less oriented core zone was revealed by morphological observations using the scanning electron microscope and the polarized optical microscope<sup>8-12</sup>. Microbeam X-ray diffraction with a 100  $\mu\text{m}$  beam diameter was applied to evaluate the microscopic orientation in the injection moulded plaques

of liquid crystalline polymers<sup>13</sup>. Polarized a.t.r./*FTi.r.* spectroscopy was used to obtain the orientation profiles in the injection moulded plaques of a liquid crystalline polymer<sup>14</sup>.

In this work, polarized *FTi.r.* microspectroscopy is applied to characterize the microscopic orientation in the extrusion moulded sheets of a liquid crystalline polymer. The orientation distribution obtained by polarized *FTi.r.* microspectra is compared with the morphological structure studied by scanning electron microscopy (SEM). In addition, we discuss the validity of *FTi.r.* microspectroscopy as a technique for analysing the microscopic structure of polymeric materials.

## EXPERIMENTAL

### *Measurements of polarized FTi.r. microspectra*

The *FTi.r.* microspectra were measured on a Perkin Elmer model 1800 *FTi.r.* spectrometer equipped with a liquid nitrogen-cooled MCT detector. One thousand scans of 4  $\text{cm}^{-1}$  resolution were averaged to achieve a sufficient signal-to-noise ratio. The microbeam radiation was obtained with a redundantly apertured i.r. microscope, IR-plan model 100 (Spectra-Tec, Inc). A sketch of the i.r. microscope is shown in *Figure 1*. The microscopic area for the spectral analysis was defined by two apertures, one before and another after the specimen.

0032-3861/92/132672-07

© 1992 Butterworth-Heinemann Ltd.

2672 POLYMER, 1992, Volume 33, Number 13

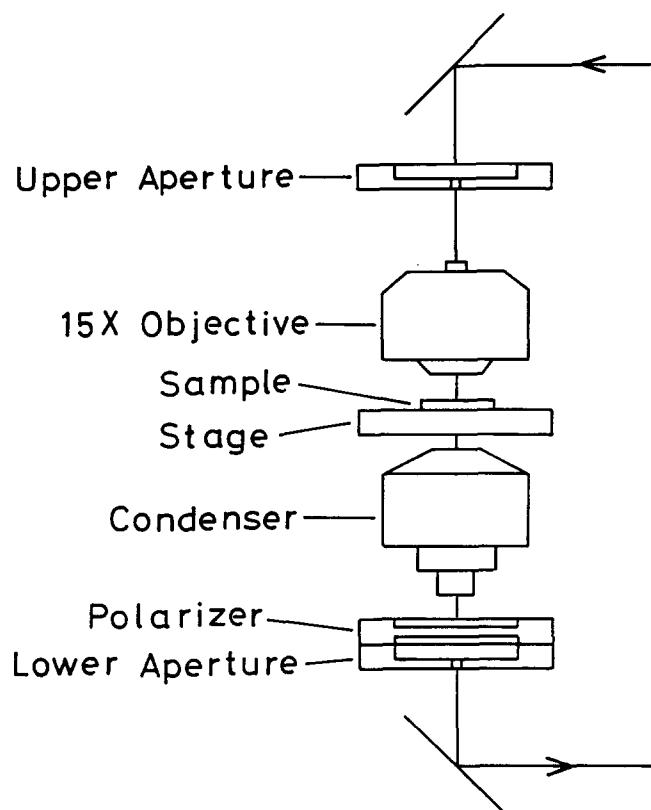


Figure 1 Sketch of i.r. microscope used in this work

I.r. radiation was focused on the sample by a 15× Cassegrainian objective, after passing through the upper aperture. A slit 0.6 mm wide and 3 mm long was used for the upper aperture, so as to form a sample image with a  $40\ \mu\text{m} \times 200\ \mu\text{m}$  dimension. The transmitted i.r. beam passed through a 10× condenser and was masked again by the lower aperture.

The linear relationship between absorbance and film thickness was verified by measuring the FTi.r. microspectra of polyethylene films 40–500  $\mu\text{m}$  thick.

The polarized FTi.r. microspectra of anisotropic samples were measured by placing a wire-grid polarizer under the condenser. The polarized FTi.r. spectra were obtained by changing the polarization direction of the polarizer. In order to examine the accuracy of polarization measurements in FTi.r. microspectroscopy, we measured the polarized microspectra of an oriented polypropylene (PP) film whose polarized spectra were already known. The oriented PP film was obtained by drawing an isotropic PP film at 135°C.

#### Sample preparation

The sample used in this work is a thermotropic liquid crystalline polymer, Ekonol E 6000 (Sumitomo Chemical Co. Ltd), consisting of 4-hydroxybenzoic acid units, biphenol units and benzene dicarboxylic acid units. The apparent viscosity<sup>15</sup> of Ekonol E 6000 was 26 Pa s at 360°C and a shear rate of 1950  $\text{s}^{-1}$ . Neither the molecular weight nor the concentration of constituent groups within the polymer is available. The polymer exhibits a broad endothermic peak owing to the crystal-mesophase transition in the temperature range of 320–360°C. Sheets of the polymer were extrusion moulded using a single-screw extruder equipped with a coat-hanger die, after pellets of the polymer were dried

at 90°C for 12 h and at 120°C for 3 h. The coat-hanger die was composed of crosshead with a diameter of 15 mm, manifold, damming zone and die lip area. The die lip area was 20 mm long in the flow direction and 120 mm wide. The gap of the die lip was adjusted at 0.75 mm. The die temperature was controlled at 355°C, 360°C or 366°C. The extruded sheets were drawn down in the molten state after leaving the die outlet, and were slowly cooled to ambient temperature. The mass output in the extrusion moulding was  $0.86\ \text{g s}^{-1}$ , and was kept constant throughout the experiment. The draw-down ratio was controlled by changing the take-up speed.

The extrusion moulded sheets were microtomed in the extrusion direction to a thickness of 10  $\mu\text{m}$ , after the sheets were embedded in an epoxy resin. The microtomed sections were used for the measurements of polarized FTi.r. microspectra.

#### Morphological observation

The extrusion moulded sheets were fractured along the extrusion direction at liquid nitrogen temperature. The fracture surfaces were coated with gold and were examined with a scanning electron microscope, Akashi model DS-130.

## RESULTS AND DISCUSSION

#### Linear relationship between absorbance and thickness

The absorption intensities of the  $\text{CH}_2$  wagging vibration of polyethylene films are plotted against the film thickness in Figure 2. Figures 2a and 2b show the integrated absorption intensity and the absorbance at the absorption peak, respectively. The integrated intensity linearly depends upon film thickness in the absorbance range of 0.0–3.0, whereas the peak intensity deviates from the linear relationship in the absorbance range above 2.5. The absorption intensities of intense absorption bands are not accurately measured near the absorption peak. The deviation from Beer's law may be attributed to the poor linearity of the MCT detector in the range of extremely low light energy.

When FTi.r. microspectroscopy is applied to micro-samples such as thin fibres and micro-spots, the light diffraction sometimes causes stray or spurious light, which reduces the photometric accuracy<sup>2,3,16,17</sup>. If the microscopic area in the large specimen is studied by FTi.r. microspectroscopy, however, the effects of light diffraction are not serious and Beer's law holds in the absorbance range of 0.0–2.5.

#### Validity of polarization measurements

Figure 3 shows the polarized FTi.r. spectra of an oriented PP film. The polarized spectra in Figure 3a are measured with an i.r. microscope equipped with a polarizer, whereas Figure 3b shows the polarized FTi.r. spectra obtained by the macroscopic transmission method. Some absorption bands exhibit large dichroism, suggesting that the polymer chains in the sample film are highly oriented in the draw direction. The polarized FTi.r. spectra measured with an i.r. microscope are in excellent agreement with those obtained by the macroscopic transmission method. The valid dichroic spectra in the microscopic area can be measured on an i.r. microscope equipped with a polarizer. The optics of

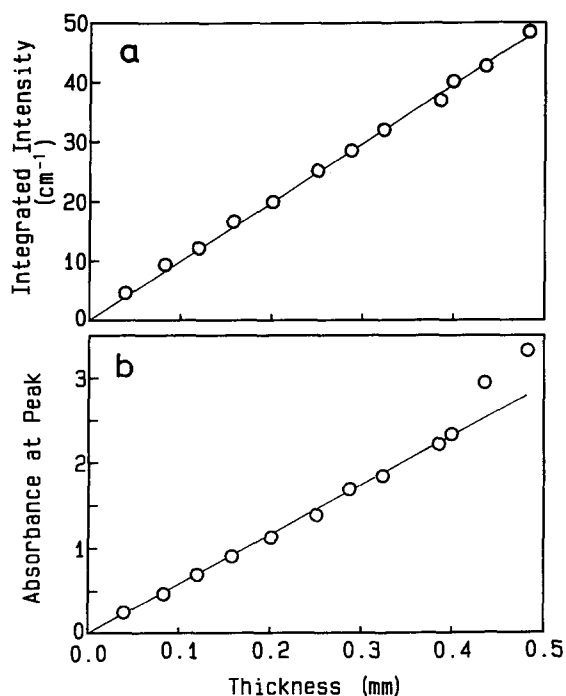


Figure 2 Plot of absorbance of the  $\text{CH}_2$  wagging vibration of polyethylene films against film thickness: (a) integrated intensity; (b) peak intensity

the i.r. microscope do not have significant effects on the polarization purity of i.r. radiation.

#### Polarized FTi.r. microspectra of the liquid crystalline polymer

Figure 4 shows the FTi.r. microspectra of the liquid crystalline polymer sheet 0.68 mm thick. The measured region is also indicated in the figure. The solid line represents the spectrum measured with polarization parallel to the extrusion direction, while the broken line is the spectrum measured with polarization parallel to the normal direction (ND). The CC stretching vibrations of aromatic rings were observed in the wavenumber region of  $1700\text{--}1350\text{ cm}^{-1}$ . By referring to the spectrum of 4-hydroxybenzoate homopolymer<sup>14,18</sup>, the i.r. bands at  $1602$ ,  $1504$  and  $1413\text{ cm}^{-1}$  are assigned to the skeletal vibrations of the benzene ring while the i.r. band at  $1492\text{ cm}^{-1}$  is ascribed to the biphenyl ring.

The microspectra in the surface region are shown in Figure 4a. The four i.r. absorption bands in the spectra exhibit large parallel dichroism, suggesting that the molecular chains are highly oriented in the extrusion direction in the surface region of the sheet. On the other hand, the FTi.r. microspectra in the central region of the polymer sheet (Figure 4b) show that the central region of the sheet is nearly isotropic. It was concluded that the extrusion moulded sheet 0.68 mm thick consisted of a highly oriented surface region and an isotropic central region.

#### Orientation profiles of the liquid crystalline polymer sheets

Figure 5 shows the microtomed sections used for the measurements of FTi.r. microspectra. The polymer sheet was microtomed parallel to the extrusion direction (ED) and normal to the sheet plane in Figure 5a, while the sheet was microtomed nearly parallel to the sheet plane in Figure 5b. The FTi.r. microspectra of the microtomed

sections were measured by changing the distance,  $X$  from the centre of the sheet. The specimen in Figure 5a gives polarized FTi.r. microspectra in the extrusion direction and in the normal direction (ND). The dichroic spectra in the extrusion direction and in the transverse direction (TD) are obtained with the section in Figure 5b. The orientation profiles of the polymer sheets were obtained by plotting the dichroic ratio of the  $1602\text{ cm}^{-1}$  band against the ratio of the distance from the centre,  $X$  to the sheet thickness,  $T$ .

The characteristics for the liquid crystalline polymer sheets studied in this work are summarized in Table 1. Sheet I and sheet II were extruded at the same extrusion condition, but sheet II was taken up at higher speed than sheet I after extrusion from the die orifice. The sheet thickness of sheet III, sheet IV and sheet V are the same as each other. The extrusion temperature was lowered in the order of sheet III, sheet IV and sheet V.

Figure 6 shows the orientation profile of sheet I. The open circles represent the ratio of absorption intensity in the extrusion direction to that in the normal direction,  $R(\text{ED}/\text{ND})$ , and the filled circles are the dichroic ratios between the extrusion direction and the transverse

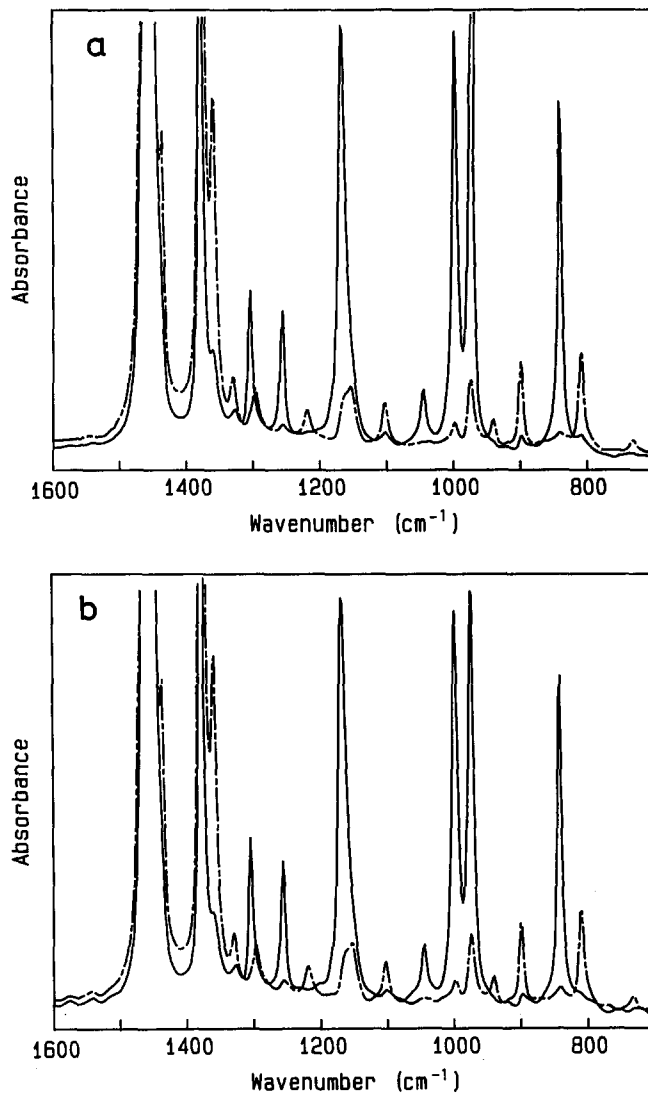
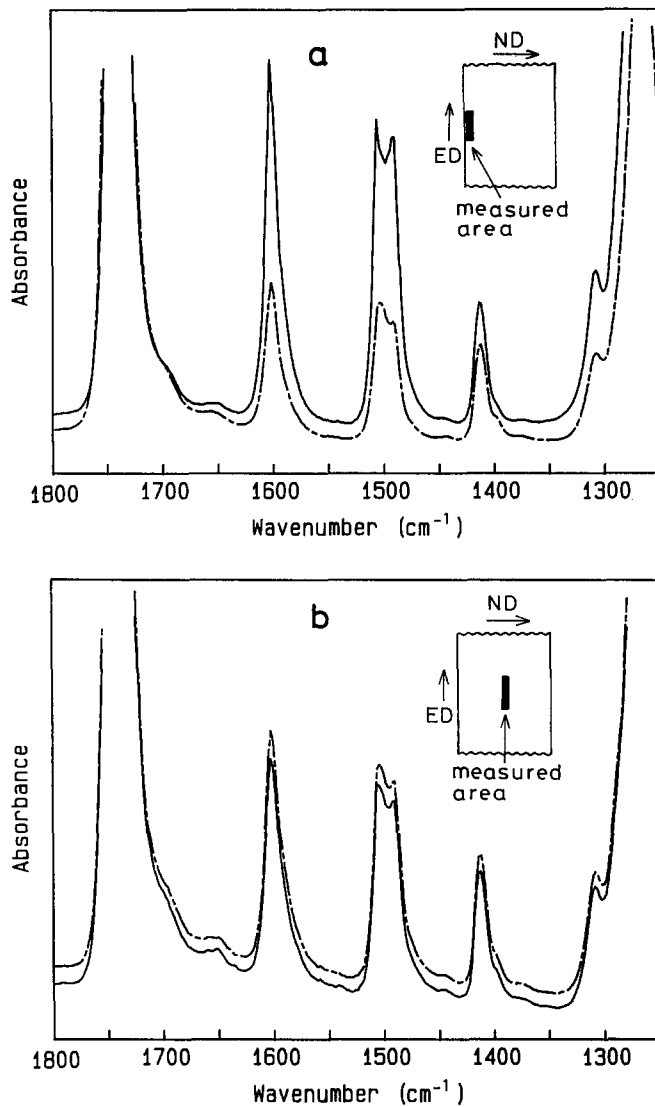
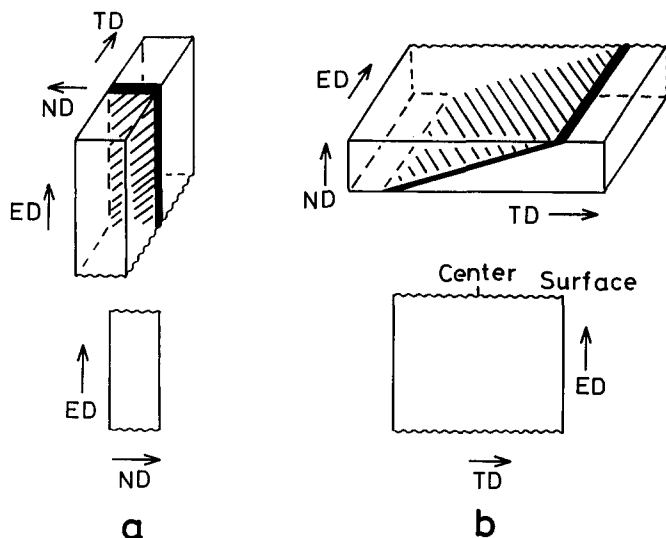


Figure 3 Polarized FTi.r. spectra of an oriented polypropylene film: (a) measured with an i.r. microscope; (b) measured by the macroscopic transmission method. (—) Parallel polarization; (---) perpendicular polarization



**Figure 4** FTi.r. microspectra of the extrusion moulded Ekonol sheet 0.68 mm thick: (a) surface region; (b) central region. (—) Parallel polarization; (---) perpendicular polarization



**Figure 5** Microtomed sections used for the measurements of FTi.r. microspectra

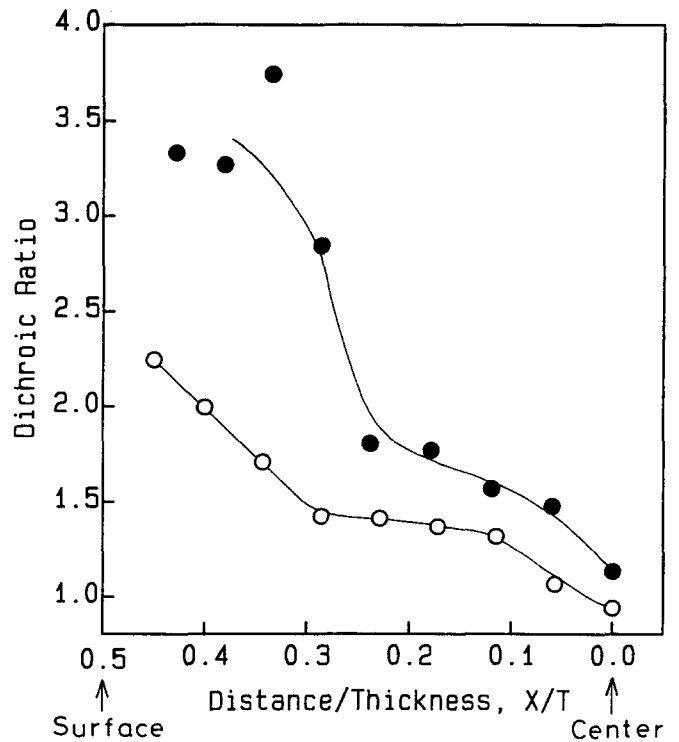


**Figure 6** Orientation profile of sheet I (thickness = 0.68 mm,  $T_E = 366^\circ\text{C}$ ): (○)  $R(\text{ED}/\text{ND})$ ; (●)  $R(\text{ED}/\text{TD})$

**Table 1** Characteristics for the liquid crystalline polymer sheets studied in this work

Sample no.	$T_E$ ( $^\circ\text{C}$ )	Draw-down ratio	Sheet thickness (mm)
Sheet I	366	1.18	0.680
Sheet II	366	3.15	0.255
Sheet III	366	2.14	0.375
Sheet IV	360	2.14	0.375
Sheet V	355	2.14	0.375

direction,  $R(\text{ED}/\text{TD})$ . In the central region of the sheet ( $X/T < 0.25$ ), the dichroic ratio increases gradually with increasing  $X/T$ , but remains below 1.8. In the surface region ( $X/T > 0.25$ ), however, the dichroic ratio increases markedly toward the surface. At any positions in the thickness direction, the value of  $R(\text{ED}/\text{TD})$  is higher than that of  $R(\text{ED}/\text{ND})$ , suggesting that the mode of molecular orientation deviates from the uniaxial orientation.

*Figure 7* shows the orientation profile of sheet II. The dichroic ratio,  $R(\text{ED}/\text{TD})$  increases from the centre to the surface, but the values of  $R(\text{ED}/\text{ND})$  are nearly constant except for one point at the centre. The values of  $R(\text{ED}/\text{TD})$  are higher than those of  $R(\text{ED}/\text{ND})$  in the central region ( $X/T < 0.3$ ), but  $R(\text{ED}/\text{ND})$  tends to exceed  $R(\text{ED}/\text{TD})$  in the surface region. The dichroic ratio in the central region is much increased in sheet II as compared with sheet I.

The orientation distribution in extrusion moulded sheets of liquid crystalline polymers is closely related to the flow characteristics of the polymer melts. The elongational flow is more effective on orienting the polymer chains than the shear flow. If the power-law model holds for the flow of the polymer melts, the

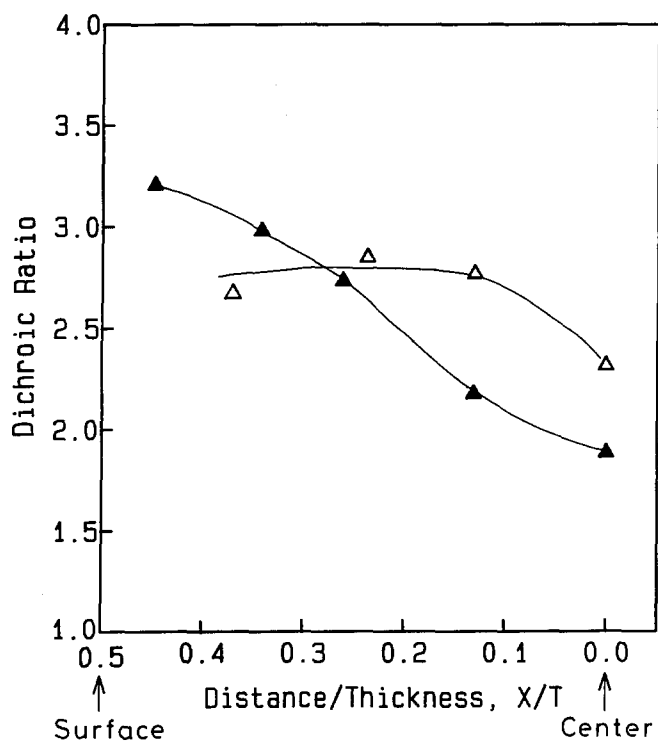


Figure 7 Orientation profile of sheet II (thickness = 0.255 mm,  $T_E = 366^\circ\text{C}$ ): ( $\Delta$ )  $R(\text{ED}/\text{ND})$ ; ( $\blacktriangle$ )  $R(\text{ED}/\text{TD})$

apparent viscosity,  $\eta$  is expressed by:

$$\eta = K\dot{\gamma}^{n-1} \quad (1)$$

where  $\dot{\gamma}$  is shear rate. The power-law exponent,  $n$  is unity for a Newtonian fluid. Based on the power law relation, the velocity profile  $V(Y/t)$  in the slit die is given by<sup>19</sup>:

$$V(Y/t) = \bar{V}((2n + 1)/(n + 1))(1 - (2Y/t)^{(n+1)/n}) \quad (2)$$

where  $Y$  is the distance from the centre of the slit die along the thickness direction and  $t$  is the gap of the die.  $V(Y/t)$  is the velocity at position  $Y$ , and  $\bar{V}$  is the averaged velocity.  $V(Y/t)$  is zero at the die wall ( $Y = t/2$ ), but has a maximum at the centre of the die ( $Y = 0$ ). After the polymer is extruded from the die, the velocity profile becomes constant along the thickness direction and the polymer melts are solidified. The draw-down ratio,  $DDR(Y/t)$  at the position  $Y$  is given by

$$\begin{aligned} DDR(Y/t) &= V_c/V(Y/t) \\ &= \overline{DDR}(n + 1)/[(2n + 1)(1 - (2Y/t)^{(n+1)/n})] \end{aligned} \quad (3)$$

where  $V_c$  is the take-up velocity of the solidified polymer, and  $\overline{DDR}$  is the averaged draw-down ratio.

The flow behaviour of liquid crystalline polymers is known to be non-Newtonian<sup>20</sup>. The shear rate dependence of viscosity was measured at  $360^\circ\text{C}$  for the liquid crystalline polymer investigated. The viscosity decreased by a factor of 0.38 with increasing shear rate<sup>15</sup> from  $1950 \text{ s}^{-1}$  to  $19500 \text{ s}^{-1}$ . A logarithmic plot of the experimental values of viscosity versus shear rate gives a straight line with a slope of  $-0.42$ , and thereby the power law exponent was obtained to be 0.58 at  $360^\circ\text{C}$ .

Figure 8 shows the distribution of draw-down ratio,  $DDR(Y/t)$  along the thickness direction, calculated for  $n = 0.58$ . The draw-down ratio increases with increasing

$Y/t$ , and the increase of draw-down ratio is accelerated in the surface region. If the averaged draw-down ratio is low, fluid elements in the surface region are stretched, but those in the central region are contracted ( $DDR(0) < 1.0$ ). At higher draw-down ratios, however, fluid elements in the central region are stretched as well as those in the surface region. The results predicted from the flow characteristics in the slit die explain the observed orientation profiles of the liquid crystalline polymer sheets.

Figure 9 shows the effects of extrusion temperature ( $T_E$ ) on the orientation profile of the liquid crystalline polymer sheets. The orientation profile of sheet III is identical to that of sheet IV, but the orientation profile of sheet V is different from the others. The dichroic ratios in sheet V are much lower than those in sheet III and sheet IV, at any positions from the centre to the surface. The degree of molecular orientation decreases as the extrusion temperature is lowered from  $360^\circ\text{C}$  to  $355^\circ\text{C}$ .

A broad endothermic peak is observed in the range  $320\text{--}360^\circ\text{C}$  on the differential scanning calorimetry (d.s.c.) thermogram, and the polymer can be extrusion moulded above  $335^\circ\text{C}$ . All crystallites in the polymer are melted above  $360^\circ\text{C}$ , but unmelted crystallites remain at  $355^\circ\text{C}$ . If the polymer is extruded above  $360^\circ\text{C}$ , the polymer chains are mobile enough to follow the flow direction. As a consequence, the highly oriented structure is formed in the sheet extruded above  $360^\circ\text{C}$ . When the extrusion temperature is lower than  $360^\circ\text{C}$ , crystallites are no longer deformed, nor orient in the flow direction. Therefore, the poorly oriented structure is developed in the sheet extruded below  $360^\circ\text{C}$ . Several researchers<sup>21-23</sup> have reported that the orientation functions in extrusion moulded liquid crystalline polymers increased as the extrusion temperature was raised. The results of this work are in agreement with those reports.

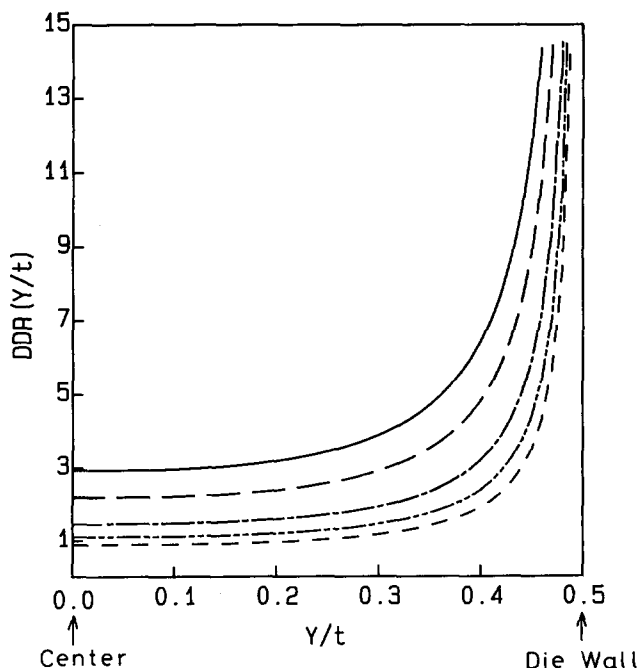
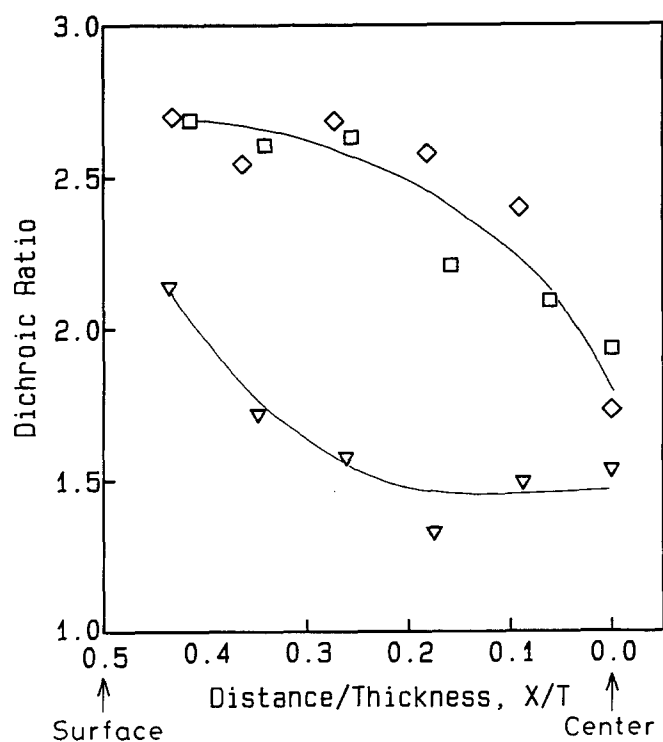
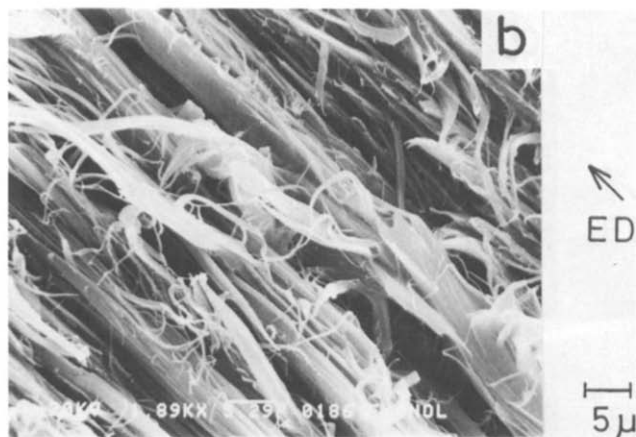
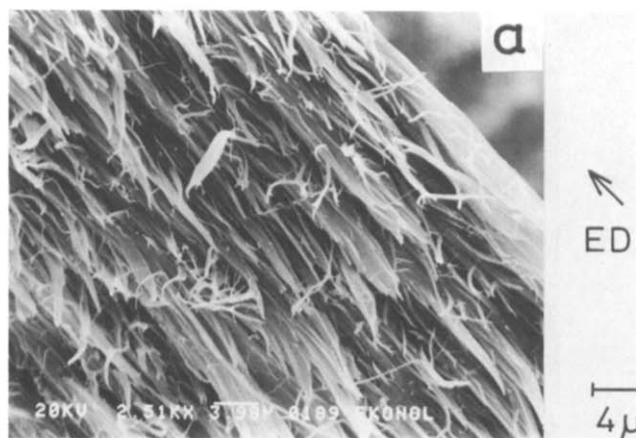


Figure 8 Distribution of draw-down ratio,  $DDR(Y/t)$ , along the thickness direction, calculated for  $n = 0.58$ : (.....)  $\overline{DDR} = 1.2$ ; (-.-.-.-)  $\overline{DDR} = 1.5$ ; (- - - -)  $\overline{DDR} = 2.0$ ; (- - - -)  $\overline{DDR} = 3.0$ ; (—)  $\overline{DDR} = 4.0$



**Figure 9** Effects of extrusion temperature ( $T_E$ ) on the orientation profiles of the liquid crystalline polymer sheets (thickness = 0.375 mm): (□) sheet III ( $T_E = 366^\circ\text{C}$ ); (◇) sheet IV ( $T_E = 360^\circ\text{C}$ ); (▽) sheet V ( $T_E = 355^\circ\text{C}$ ). The dichroic ratio  $R(\text{ED}/\text{ND})$  is shown



**Figure 11** SEM photographs of the fracture surface of sheet II: (a) surface region; (b) central region

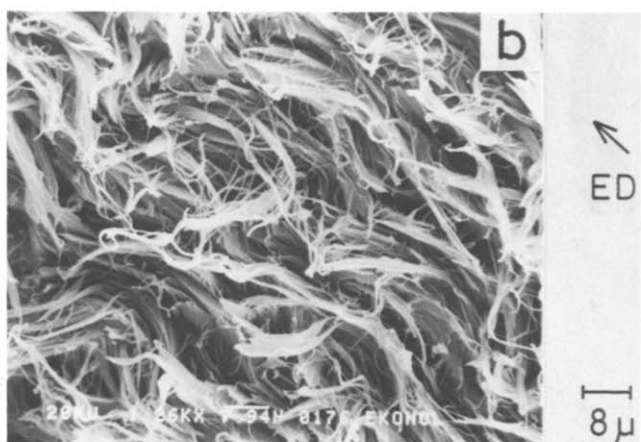
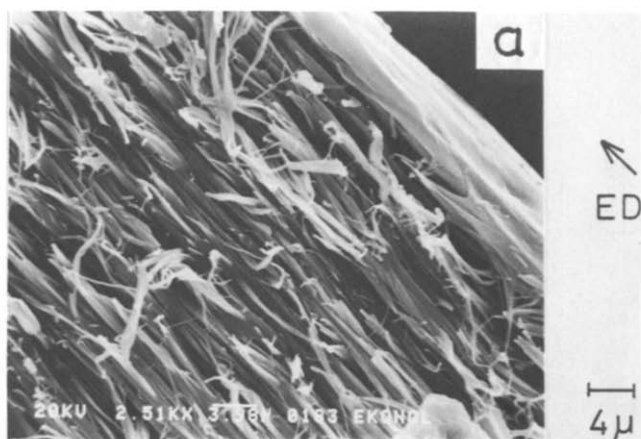


**Figure 10** SEM photographs of the fracture surface of sheet I: (a) surface region; (b) central region

#### Fracture surface morphology

Figure 10 shows the SEM photographs of the fracture surface of sheet I. Fibrils 0.5–2 μm in diameter are developed in both central and surface regions of sheet I. Straight fibrils are highly oriented in the extrusion direction in the surface region (Figure 10a), whereas curved fibrils are poorly oriented in the central region (Figure 10b). In the fibrils, the molecular chains tend to align in the direction of the fibril axis. The low degree of molecular orientation in the central region of sheet I (Figure 7) is attributed to the poor orientation of the fibril axis.

Figure 11 shows the SEM photographs of the fracture surface of sheet II. Fibrils are highly oriented in the extrusion direction in both central and surface regions. The fibrils in the surface region are thinner than those in the central region.

Figure 12 shows SEM photographs of the fracture surface of sheet V. Although the sheet tends to cleave along the extrusion direction, the fibrillar structure is not fully developed in sheet V. When the extrusion temperature is lower than 360°C, unmelted crystallites restrict fibre structure formation. A lumpy structure is observed in the central region of sheet V, while the structure in the surface region is configured in the aggregation of bundles. The morphological features in sheet V coincide with the low degree of molecular orientation in the orientation profile (Figure 9).

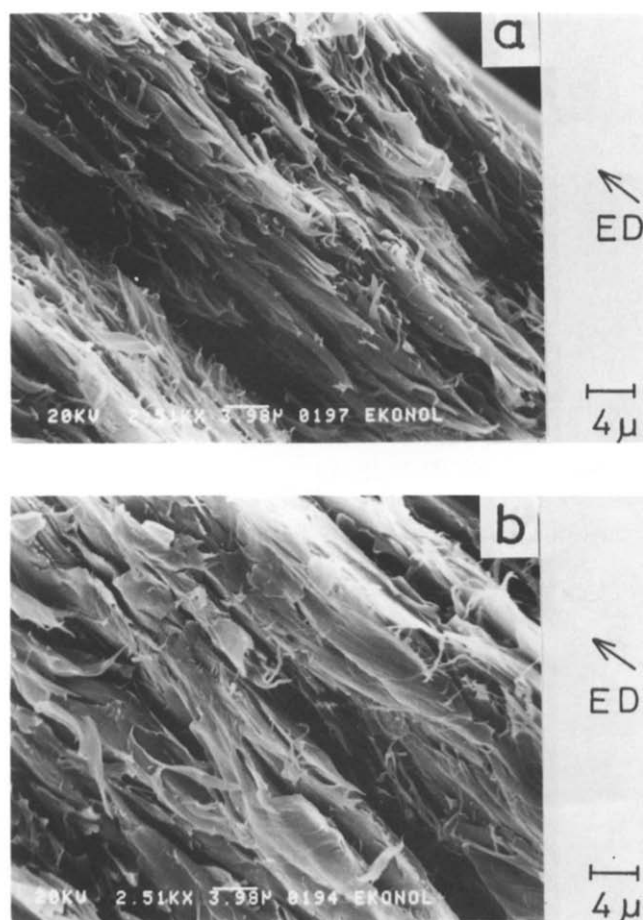


Figure 12 SEM photographs of the fracture surface of sheet V: (a) surface region; (b) central region

## CONCLUSIONS

It was demonstrated that polarized FTi.r. microspectroscopy using a redundantly apertured i.r. microscope was useful for characterizing the microscopic orientation of oriented polymers. A good linear relationship between absorbance and thickness was achieved in the absorbance range of 0.0–2.5. The polarization properties of FTi.r. microspectra were shown to be accurately measured with an i.r. microscope equipped with a polarizer.

The orientation profiles in the sheets of the liquid crystalline polymer were obtained by polarized FTi.r. microspectroscopy. The orientation profiles were discussed in relation to the fracture surface morphology.

When the extrusion temperature is higher than 360°C, the fibrillar structure is developed in the extrusion moulded sheets. In the sheet 0.68 mm thick (sheet I), the molecular chains are poorly oriented in the central region, but the degree of orientation increases on approaching the surface. In the thinner sheet (sheet II), the degree of orientation in the surface region is also higher than that in the central region, but the molecular orientation in the central region is much improved in sheet II as compared with sheet I.

When the extrusion temperature is lower than 360°C, unmelted crystallites restrict the formation of fibrillar morphology. The degree of microscopic orientation in the sheet extruded at 355°C (sheet V) is lower at all positions from the centre to the surface than that in the sheet extruded at higher temperatures (sheet III and sheet IV).

## REFERENCES

- 1 Schearer, J. C. and Peters, D. C. ASTM Spec. Tech. Publ. 1987, No. 949, 27
- 2 Miseo, E. V. and Guilmett, L. W. ASTM Spec. Tech. Publ. 1987, No. 949, 97
- 3 Chase, D. B. ASTM Spec. Tech. Publ. 1987, No. 949, 4
- 4 Bartick, E. G. ASTM Spec. Tech. Publ. 1987, No. 949, 64
- 5 Reffner, J. A., Messerschmidt, R. G. and Coates, J. P. *Microbeam Anal.* 1987, **22**, 180
- 6 Mirabella, Jr, F. M. ASTM Spec. Tech. Publ. 1987, No. 949, 74
- 7 Chase, D. B. 'Infrared Microspectroscopy', Marcel Dekker, New York, 1987, p. 93
- 8 Shimamura, K., White, J. L. and Feller, J. F. *J. Appl. Polym. Sci.* 1981, **26**, 2165
- 9 Ide, Y. and Ophir, Z. *Polym. Eng. Sci.* 1983, **23**, 261
- 10 Sawyer, L. C. and Jaffe, M. *J. Mater. Sci.* 1986, **21**, 1897
- 11 Weng, T., Hiltner, A. and Baer, E. *J. Mater. Sci.* 1986, **21**, 744
- 12 Takeuchi, Y., Shuto, Y. and Yamamoto, F. *Polymer* 1988, **29**, 605
- 13 Blundell, D. J., Chivers, R. A., Curson, A. D., Love, J. C. and MacDonald, W. A. *Polymer* 1988, **29**, 1459
- 14 Pirnia, A. and Sung, C. S. P. *Macromolecules* 1988, **21**, 2699
- 15 Sumitomo Chemical Co. Ltd, personal communication
- 16 Ryan, J., Kwiatkoski, J. and Reffner, J. A. *Am. Lab. (Fairfield, Conn.)* 1989, **21**, 26
- 17 Messerschmidt, R. G. *Microbeam Anal.* 1987, **22**, 169
- 18 Kaito, A., Kyotani, M. and Nakayama, K. *Macromolecules* 1991, **24**, 3244
- 19 Han, C. D. 'Rheology in Polymer Processing', Academic, New York, 1976, p. 109
- 20 Wissbrun, K. F. *Faraday Discuss. Chem. Soc.* 1985, **79**, 161
- 21 Sugiyama, H., Lewis, D. N., White, J. L. and Feller, J. F. *J. Appl. Polym. Sci.* 1985, **30**, 2329
- 22 Muramatsu, H. and Krigbaum, W. R. *J. Polym. Sci., Polym. Phys. Edn.* 1986, **24**, 1695
- 23 Chen, G. Y., Cuculo, J. A. and Tucker, P. A. *J. Polym. Sci., Polym. Phys. Edn.* 1988, **26**, 1677